



Methylmercury dynamics at the upland-peatland interface: Topographic and hydrogeochemical controls

Carl P. J. Mitchell,^{1,2} Brian A. Branfireun,² and Randall K. Kolka³

Received 14 January 2008; revised 13 November 2008; accepted 2 December 2008; published 5 February 2009.

[1] Peatlands are important environments for the transformation of atmospherically deposited inorganic mercury into the bioaccumulative form, methylmercury (MeHg), which may accumulate in downstream aquatic biota, particularly in fish. In recent research, it was suggested that MeHg production and/or accumulation “hot spots” at the upland-peatland interface were the result of upland fluxes of sulfate and labile dissolved organic carbon (DOC) into the peatland margin. Along the upland-peatland interface, spatial heterogeneity of “hot spots” was thought to be a result of variations in upland hydrologic interaction with the peatland margin. This hypothesis was tested in this study. Pore water MeHg, sulfate, and dissolved organic carbon (DOC) concentrations were compared in peatland plots at the base of both topographically concave and linear upland subcatchments in Minnesota. Subcatchment contributing areas were 3–8 times larger in the peatland plots adjacent to areas of concave upland topography. Peat pore water MeHg concentrations were significantly higher in these plots. Fluxes of water, sulfate, and dissolved organic carbon (DOC) from the upland hillslope into the peatland margin were also generally much larger than those from below areas of concave upland topography. Taken together, these results suggest that watershed geomorphology plays an important role in controlling chemical fluxes into peatland margins and consequently MeHg production and accumulation. It may thus be possible to delineate areas of high MeHg production and/or accumulation in certain watersheds by using high-resolution topographic data. The resulting MeHg “hot spots” may be important for locally foraging biota and for downstream loading, especially in the spring and fall.

Citation: Mitchell, C. P. J., B. A. Branfireun, and R. K. Kolka (2009), Methylmercury dynamics at the upland-peatland interface: Topographic and hydrogeochemical controls, *Water Resour. Res.*, 45, W02406, doi:10.1029/2008WR006832.

1. Introduction

[2] Recent research has introduced the concept of disproportionately high rates of biogeochemical processing in discrete locations in ecosystems, referred to as biogeochemical “hot spots” [McClain *et al.*, 2003]. Most hot spots in the landscape occur where a biogeochemical reaction is fuelled by the hydrologic delivery of an electron acceptor to a zone with a suitable organic substrate, either derived in situ or from another hydrologic flow path [McClain *et al.*, 2003]. Hydrologic flow paths appear to be a major control on the functioning of these biogeochemical hot spots. For example, Hedin *et al.* [1998] found that denitrification hot spots occurred at the confluence of two disparate flow paths, one shallow, horizontal, subsurface flow path high in electron donors, and another vertical upwelling of deeper groundwater high in electron acceptors. Vidon and Hill [2004] found that proxy measures of hydrology such as slope,

sediment texture, and the depth to confining layers were useful predictors in determining the location of denitrification hot spots in riparian zones. All of these studies have indicated that a thermodynamic perspective, considering the interaction of electron acceptors and donors with microbial communities, as well as an understanding of physical landscape factors, such as geomorphic structures and topography are important in understanding the occurrence of denitrification hot spots. Until very recently, the elements and ecosystem interfaces studied with respect to biogeochemical hot spots have been narrowly focused.

[3] Recent research has expanded the concept of biogeochemical hot spots by investigating the occurrence of net methylmercury (MeHg) production and/or accumulation hot spots in peatlands [Mitchell *et al.*, 2008b]. Delineating areas where MeHg is rapidly produced is of particular interest because MeHg is a potent neurotoxin that bioaccumulates in wildlife and humans [Ratcliffe *et al.*, 1996]. The production of MeHg is enhanced by sulfate [Gilmour *et al.*, 1992; Benoit *et al.*, 2003] because sulfate-reducing bacteria are stimulated by these inputs and methylate mercury as a by-product of sulfate reduction [Compeau and Bartha, 1985]. Previous research has shown that the addition of sulfate to peatlands significantly increases the production of MeHg [Branfireun *et al.*, 1999, 2001; Jeremiason *et al.*, 2006]. The purpose of sulfate dosing experiments such as these was to

¹Department of Physical and Environmental Sciences, University of Toronto at Scarborough, Toronto, Ontario, Canada.

²Department of Geography, University of Toronto at Mississauga, Mississauga, Ontario, Canada.

³Northern Research Station, U.S. Department of Agriculture Forest Service, Grand Rapids, Minnesota, USA.

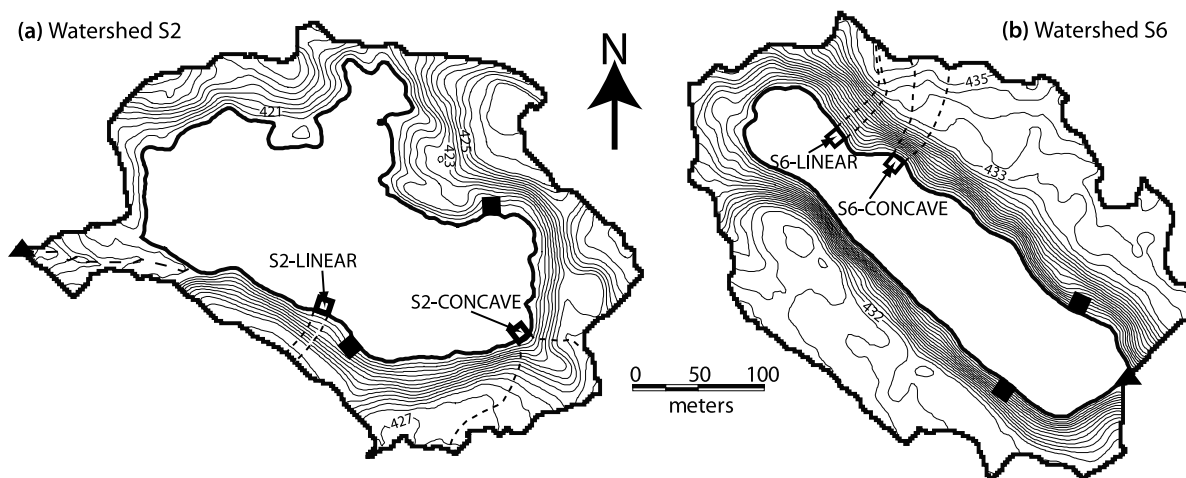


Figure 1. Study watersheds S2 and S6. Topographic contours are meters above mean sea level and are at 0.5-m intervals. Open squares represent the peatland sampling plot size and locations below areas of both linear and concave upland topography in each watershed. Upland contributing areas, based on surface topography, are delineated above each plot. Solid squares indicate the placement of previously installed upland runoff collectors [see *Timmons et al.*, 1977]. Solid triangles indicate the watershed outlets.

determine the effects of increased atmospheric sulfate pollution and deposition on the methylation of mercury, but did not specifically investigate this from a spatial perspective. In recent work, the understanding of mercury methylation in peatlands has been furthered by showing the following: (1) Hot spots of mercury methylation in peatlands dominantly occur in the interface zone between uplands and peatlands [*Mitchell et al.*, 2008b], and (2) Mercury methylation in peatlands is controlled by the availability of sulfate and a labile carbon source that when combined result in higher rates of net MeHg production than with sulfate alone [*Mitchell et al.*, 2008a]. A suitable carbon source is dissolved organic matter (DOM) leached from upland plant litter. The purpose of the current study is, in part, to explain these findings and to investigate the importance of the upland-peatland hydrologic connection to the production of MeHg in peatlands.

[4] In catchments at the Marcell Experimental Forest in northern Minnesota, subsurface flow paths tend to follow surface topography [*Nichols and Verry*, 2001]. Much hydrologic research has postulated that under such conditions, topographic slope and upland contributing areas may be good predictors of hydrologic flow path [*Anderson and Burt*, 1978; *Quinn et al.*, 1991]. In some cases, physical measurements and modeling have demonstrated that upland hydrologic fluxes into wetlands are not uniform along the outer wetland perimeter and that multiple hot spots of lateral input may occur [*Brown et al.*, 2003]. In this study, we hypothesized that since subsurface flow paths tend to follow surface topography in these watersheds, concave upland topographic forms will result in more convergent flow from larger upland subcatchment areas than will convex or linear upland topographic forms. More nutrient and carbon laden upland runoff will then be delivered to discrete locations at the upland-peatland margin below concave upland topographies. Once this energy-laden upland runoff mixes with anoxic pore water within the peatland, high rates of sulfate reduction and coincidentally, Hg methylation will occur.

Testing this hypothesis is a critical first step in linking the physical characteristics of a watershed to the extent and magnitude of MeHg production zones at larger landscape scales.

2. Methods

2.1. Study Sites

[5] This study took place in two peatlands (S2 and S6; Figure 1) at the Marcell Experimental Forest (MEF) in north central Minnesota (47°32'N, 93°28'W), U.S.A. These study sites are two of seven small experimental watersheds at MEF. The glaciated terrain of the area is typical of the western Great Lakes region and is characterized by rolling upland topography with numerous small lakes and wetlands. Peat soils were derived from sphagnum mosses and herbaceous plants over limnic materials and glacial sediments, which accumulated in an ice block depression [*Verry and Timmons*, 1982]. Peat soils are up to 9 m deep. Deep upland soils were formed from glacial drift. Ely Greenstone and granitic bedrock lie approximately 40 m below the peatland surface. Above this is ~5 m of Winnipeg Drift (limestone, sand, and gravel in a clay matrix). The Winnipeg Drift is topped by approximately 30 m of Rainy Drift (medium sands below a sandy clay loam). Nearer the surface, 1–2 m of low-permeability Koochiching Drift (clay loam; B horizon) lies above the Rainy Drift. The Koochiching Drift is then capped by approximately 30–50 cm of more permeable aeolian sandy loam (A horizon). The upper organic surface horizon (O horizon) is 2 to 7 cm depth. The regional water table lies below the peatland bottom in S6, but in some years may slightly intersect the deepest peat in S2. Thus local hydrologic interactions dominate between upland and peatland in these watersheds. During wet periods, interflow in the upland soil moves through the shallow A horizon, along the upper boundary of the low-permeability B horizon toward the peatland in each watershed [*Timmons et al.*, 1977].

[6] Peatland S2 is a roundish, 3.0 ha basin bog, surrounded by 6.2 ha of upland forest and peatland S6 is an elliptical 2.4 ha basin bog, surrounded by a 6.5 ha upland forest. Peatland vegetation is similar in both study areas and consists of a mat of mosses (*Sphagnum* spp.) with an overstory of *Picea mariana* (black spruce) and an understory of ericaceous shrubs such as *Ledum groenlandicum* (labrador tea) and *Chamaedaphne calyculata* (leatherleaf), with scattered sedges (*Carex* spp.). Both peatlands have a distinctive outer edge, the upland-peatland interface (synonymous with the peatland lagg), which is hydrologically influenced by both the peatland and the surrounding uplands [Urban *et al.*, 1989; Kolka *et al.*, 2001]. The upland to peatland boundary can be somewhat dynamic, but is defined by the start of surface or near-surface mineral soils on the upland side and an increase in peat depth on the peatland side. The upland-peatland interface zone is also slightly topographically depressed, resulting in more surface saturation compared to the inner peatland. Visually, vegetation is considerably denser and the species more diverse at the upland-peatland interface compared to the central peatland. *Betula papyrifera* (paper birch), *Larix laricina* (tamarack), *Alnus rugosa* (speckled alder), and various semiaquatic flowering plant species are found within the upland-peatland interface. The upland-peatland interface of peatland S6 is larger (10–15 m wide) and more continuous than the upland-peatland interface of peatland S2 (1–10 m wide). Upland vegetation differs between the two catchments. Upland vegetation in S2 is composed mainly of *Populus tremuloides* (trembling aspen) and *B. papyrifera*. The upland of S6 was clear-cut in 1980 to convert the *P. tremuloides* forest to *Picea glauca* (white spruce) and *Pinus resinosa* (red pine). Climate at MEF is characterized as subhumid continental. January and July air temperatures were -16°C and 20°C , respectively during the 2005 study year and total precipitation for 2005 was 672 mm. 2005 temperatures and precipitation were typical for this region, but precipitation was approximately 100 mm below average [Verry and Timmons, 1982; US Forest Service, unpublished data, 2008].

2.2. Field Sampling

[7] Two sampling grids (12 points in an approximate 10×10 m square) were established in each peatland, at the upland-peatland interface (Figures 1 and 2). In each peatland, sampling grids were established both: (1) below areas of concave upland topography (S2-CONCAVE and S6-CONCAVE), and (2) below areas of linear, or slightly convex upland topography (S2-LINEAR and S6-LINEAR). Boardwalks were built before sampling to reduce disturbance of these sites. Samples were taken in the spring (early June), summer (early August) and fall (early October) of 2005.

[8] Pore water samples were obtained over an integrated depth of 2.5 to 7.5 cm below the water table using a Teflon piezometer with a 5 cm slotted head and a peristaltic pump as in the work of Mitchell *et al.* [2008b] using ultraclean techniques [Gill and Fitzgerald, 1987]. Concomitant with pore water sampling, runoff samples were collected from the V notch weirs located at the outlets of the watersheds (Figure 1). When possible, samples were also obtained from upland wells and established upland runoff collectors (Figures 1 and 2) [see Verry and Timmons, 1982]. All samples were filtered in the field using a peristaltic pump and acid-washed Teflon tubing with ashed $0.7 \mu\text{m}$ glass

fiber filters in precleaned and acid-washed Teflon in-line filter holders. Samples for total mercury (THg) and MeHg analyses were collected in polyethylene terephthalate glycol (PETG) bottles, acidified to 0.5% immediately with concentrated ultrapure hydrochloric acid (HCl), double bagged in ziplock bags, and kept in dark plastic bags in a cold cooler until return from the field. Filtered samples were also collected in high-density polyethylene (HDPE) bottles for analysis of dissolved organic carbon (DOC) and sulfate and kept in a cold cooler until return from the field.

2.3. Hydrologic Measurements

[9] Discharge from each catchment was measured below the outlets over 120° V notch weirs using continuous recording stream gauges. Discharge data were averaged daily. Catchments S2 and S6 have been monitored for discharge since 1961 and have well-established stage-discharge relationships.

[10] At each upland-peatland interface, the direction of the hydraulic flux was measured by monitoring the water table slope between wells (~ 1 m length) on either side of this boundary, with the assumption that the major flux of water from upland to peatland was horizontal (Figure 2). Water table measurements were made weekly using an electronic water sensor and the relative elevation of each well was measured using a Sokkia[®] Set 4B Total Station (Sokkia Corporation, Olathe, KS). Multiple measurements of saturated hydraulic conductivity (K_{sat}) were made in the upland areas above each studied upland-peatland interface plot. Measurements were made within the A horizon (through which interflow occurs) using a Guelph permeameter (Soilmoisture Equipment Corporation, Santa Barbara, CA). The magnitude of the hydraulic flux ($\text{m}^3 \text{wk}^{-1}$) was estimated across the 10 m wide interface plots using Darcy's Law, assuming a horizontal flux only. This hydraulic flux was then multiplied by chemical concentrations in upland saturated soil to determine the mass flux of sulfate and DOC into the peatland.

2.4. Analytical Methods

[11] THg and MeHg analyses were performed in a Class 100 cleanroom at the University of Toronto using U.S. Environmental Protection Agency (USEPA) Methods 1631 [USEPA, 2002] and 1630 [USEPA, 2001]. MeHg concentration was determined by aqueous phase ethylation [Bloom, 1989] and cold vapor atomic fluorescence spectroscopy (CVAFS) on a Tekran[®] 2500 (Tekran Instrument Corporation, Knoxville, TN) following distillation [Horvat *et al.*, 1993]. Recovery of a MeHg spike was $98 \pm 12\%$ ($n = 30$), replication of duplicates was $8 \pm 5\%$ ($n = 18$ pairs), and the detection limit, calculated as 3 standard deviations of distillate blanks, was 0.02 ng l^{-1} ($n = 17$). THg concentration in water was determined using a Tekran[®] model 2600 CVAFS mercury detector with automated sampler through two-stage gold trap amalgamation and reduction by SnCl_2 . The day prior to analysis, 1 mL of BrCl was added to 40 mL of sample. Recovery of a THg spike was $100 \pm 5\%$ ($n = 12$), replication of duplicates was $1.9 \pm 1.4\%$ ($n = 30$ pairs), and the detection limit was 0.20 ng l^{-1} ($n = 18$).

[12] Sulfate was analyzed on a model DX 500 Dionex[®] ion chromatography system with a self-regenerating suppressor (Dionex Corporation, Sunnyvale, CA) at the University of Toronto. DOC was analyzed on a Shimadzu[®] 5050

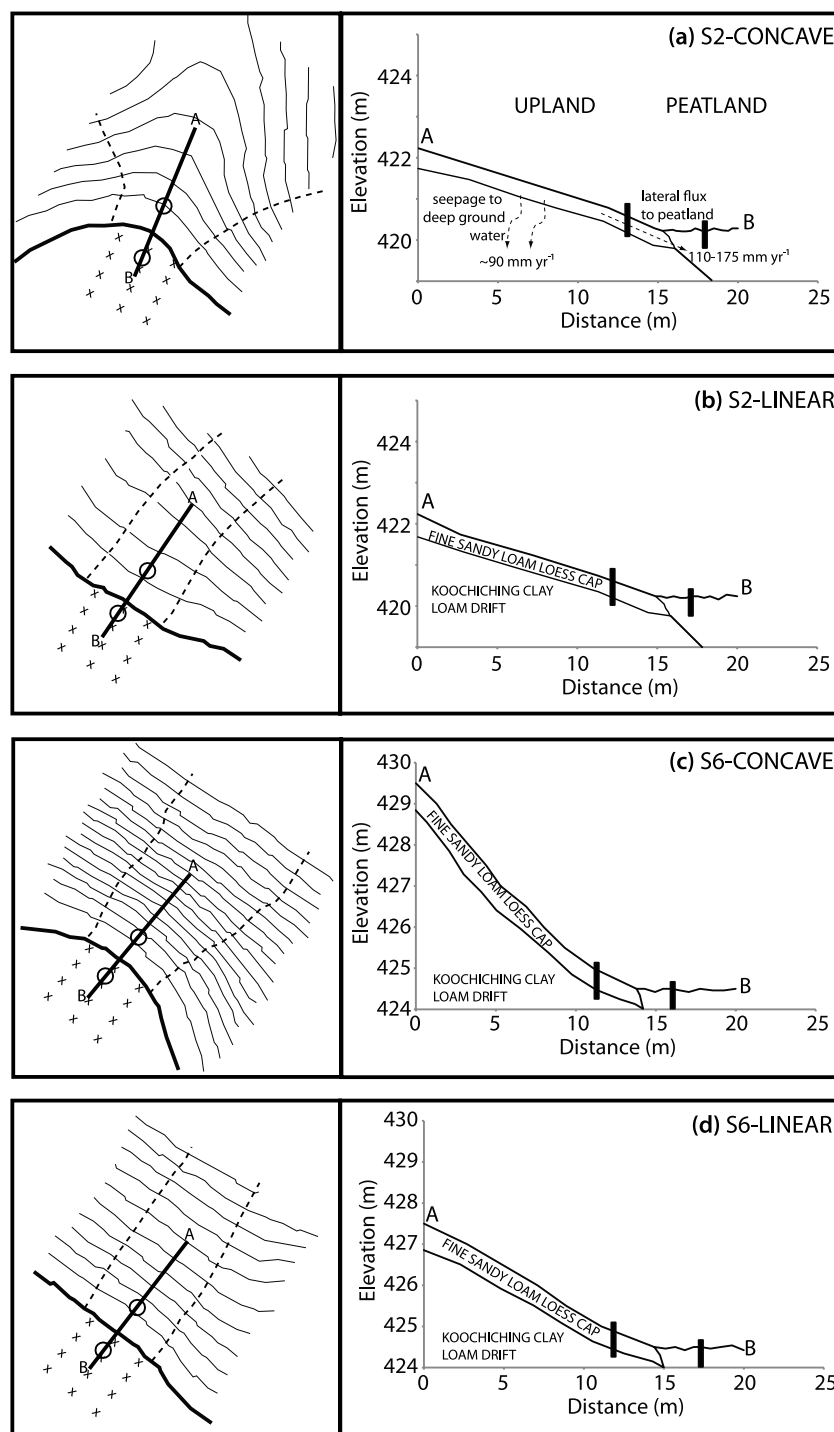


Figure 2. (left) Upland-Peatland transects, showing location of wells (open circles) and peatland sampling points (crosses). (right) Slope profiles from A–B transects delineated on the left side, showing near-surface soil horizons. Upland runoff flows into the peatland above the slowly permeable Koochiching clay loam soils. In Figure 2a, approximate annual upland water fluxes are delineated and presumed to be similar for all transects [hydrologic data from *Timmons et al.*, 1977; *Nichols and Verry*, 2001].

Total Organic Carbon Analyzer (Shimadzu Corporation, Kyoto, Japan), employing high-temperature (680°C) catalytic combustion at McGill University. Three to six injections of each sample were performed until coefficients of variations were less than 5%.

2.5. Spatial Mapping and Statistical Methods

[13] High-resolution topographic data from both watersheds were obtained from light detection and ranging (LiDAR) flights over the MEF. To facilitate repeated measurements of the same sample points throughout the year, all sampling points were flagged and accurately

georeferenced using a Sokkia[®] Set 4B Electronic Total Station. Pore water chemical concentrations were mapped and spatially interpolated using kriging methods in Surfer[®] mapping software (Golden Software, Golden, CO). Statistical comparison of sample groups was conducted using non-parametric tests since data were not normally distributed. Significant differences between two groups (i.e., plots below different upland topographic configurations in a single watershed) were investigated using the Mann-Whitney U test, whereas significant differences among multiple groups (i.e., all plots in both watersheds) were investigated using the Kruskal-Wallis analysis of variance (ANOVA). All tests were conducted using Statistica[®] software (Statsoft Inc., Tulsa, OK). Because of the high level of variability previously observed for chemical concentrations in these peatlands [Mitchell *et al.*, 2008b], the results of statistical tests were judged for significance at $p < 0.10$.

3. Results and Discussion

3.1. Soil Profiles, Topography, and Concept of Hydrologic Exchange Between Upland and Peatland

[14] In previous work in these watersheds, researchers have found significant runoff from uplands into the peatlands, but have not investigated this on a spatially distributed basis [Timmons *et al.*, 1977; Verry and Timmons, 1982]. Timmons *et al.* [1977] found that upland interflow, outside of the snowmelt period, specifically into the S2 peatland, averaged 57 mm (based on upland area) over three years of study (8.9% of average 640 mm of rain over the same period). On an annual basis, another 51 to 125 mm of runoff may also occur during the snowmelt period [Timmons *et al.*, 1977]. Similar data is not available for upland runoff from S6, but it is likely slightly less as indicated by lower runoff yields during snowmelt [Mitchell *et al.*, 2008c].

[15] Overall, the horizontal flow of water in the uplands of these watersheds is dependent on the low-permeability B horizon at approximately 30 cm in both watersheds (Figure 2) [Timmons *et al.*, 1977; Verry and Timmons, 1982]. As a result of this low-permeability layer, an episodic, perched water table leads to local-scale lateral subsurface flow and interactions between shallow subsurface runoff from the upland and near-surface waters from the peatland at the upland-peatland interface. This is supported by measurement of a near-surface water table that is well above that of the regional water table. At the peatland margins, vertical hydraulic gradients tend to be downward with losses from the upland-peatland interface to deep groundwater. Some seepage from upland hillslope soils to deep groundwater does occur, but vertical seepage is less than interflow. The loss of upland water via unsaturated flow below the A–B horizon interface has been estimated as 90 mm a^{-1} whereas interflow ranges from approximately $110\text{--}175 \text{ mm a}^{-1}$ (Figure 2) [Timmons *et al.*, 1977; Nichols and Verry, 2001]. Thus, as the lateral movement of subsurface water dominates and generally follows topography, larger upland subcatchments should produce more runoff that interacts with peatland margins.

[16] Topographically defined upland subcatchment areas below peatland sampling plots in both watersheds differed by 3–8.5 times, depending on whether upland topographies were linear or concave (Figure 1). In watershed S2, the

subcatchment area above S2-LINEAR was 410 m^2 whereas above S2-CONCAVE, it was 3500 m^2 . In watershed S6, the subcatchment area above S6-LINEAR was 550 m^2 whereas above S6-CONCAVE, it was 1700 m^2 . Upland slopes near the upland-peatland interface of each plot also differed (Figure 2). Upland slopes in watershed S6 were steeper than in S2. Both of the upland slopes measured in watershed S2 were similar. The upland slope above S6-CONCAVE was the steepest among those measured. Conceptually, with all else being equal (i.e., K_{sat} , vertical seepage, soil water chemical concentrations), and presuming as in previous work [Verry and Timmons, 1982; Nichols and Verry, 2001] that upland flow paths generally follow topography, more flow paths should converge at the upland-peatland interface when upland subcatchments are concave, and are thus larger than topographically linear upland subcatchments. Where upland slopes are greater, hydraulic gradients may be larger, also contributing to more flow. Thus our hypothesis is that runoff will undoubtedly be greater into plots S2-CONCAVE and S6-CONCAVE, compared to S2-LINEAR and S6-LINEAR, resulting in higher concentrations of MeHg in the S2-CONCAVE and S6-CONCAVE upland-peatland interface plots.

3.2. Pore Water Chemistry at the Upland-Peatland Interface

[17] Pore water MeHg concentrations were significantly higher in the peatland plots situated below topographically concave uplands (Figure 3). After lumping seasonal samples together, pore water MeHg concentrations were significantly greater in S6-CONCAVE than in S6-LINEAR ($p < 0.001$) and in S2-CONCAVE compared to S2-LINEAR ($p = 0.076$). During individual sampling periods, differences between the two types of plots in peatland S2 were significant only in the spring ($p = 0.041$). Differences in the summer ($p = 0.165$) and fall ($p = 0.538$) were not significant. In peatland S6, differences were significant in both the spring ($p = 0.0094$) and fall ($p = 0.0007$), but not in the summer ($p = 0.462$). Coincidentally, spring and fall are the two seasons wherein upland interflow is most likely to occur [Kolka *et al.*, 2001]. The greatest mean MeHg concentrations were observed in S6-CONCAVE, above which the upland slope was steepest of all studied sites. These patterns support our hypothesis that the production and/or accumulation of MeHg are/is most pronounced in peatland areas adjacent to upland concave topographies.

[18] Pore water MeHg concentrations had more distinguishable spatial patterns at the upland-peatland interface plots situated below upland areas with concave topography. Although spatial patterns of pore water MeHg concentration were different between watersheds for this type of upland-peatland configuration, concentrations were highest near the upland interface in both plots (Figure 3). The principal difference between the plots was that a band of high MeHg concentration in pore waters at S6-CONCAVE occurred at a small distance from the actual interface ($\sim 3 \text{ m}$) whereas the highest concentrations in S2-CONCAVE were found directly adjacent to the upland-peatland interface.

[19] Differences in pore water MeHg concentration between the two peatland plots below areas of concave upland topography cannot be explained in relation to the magnitude of upland subcatchment area or concavity. The subcatchment area above S2-CONCAVE was approximately

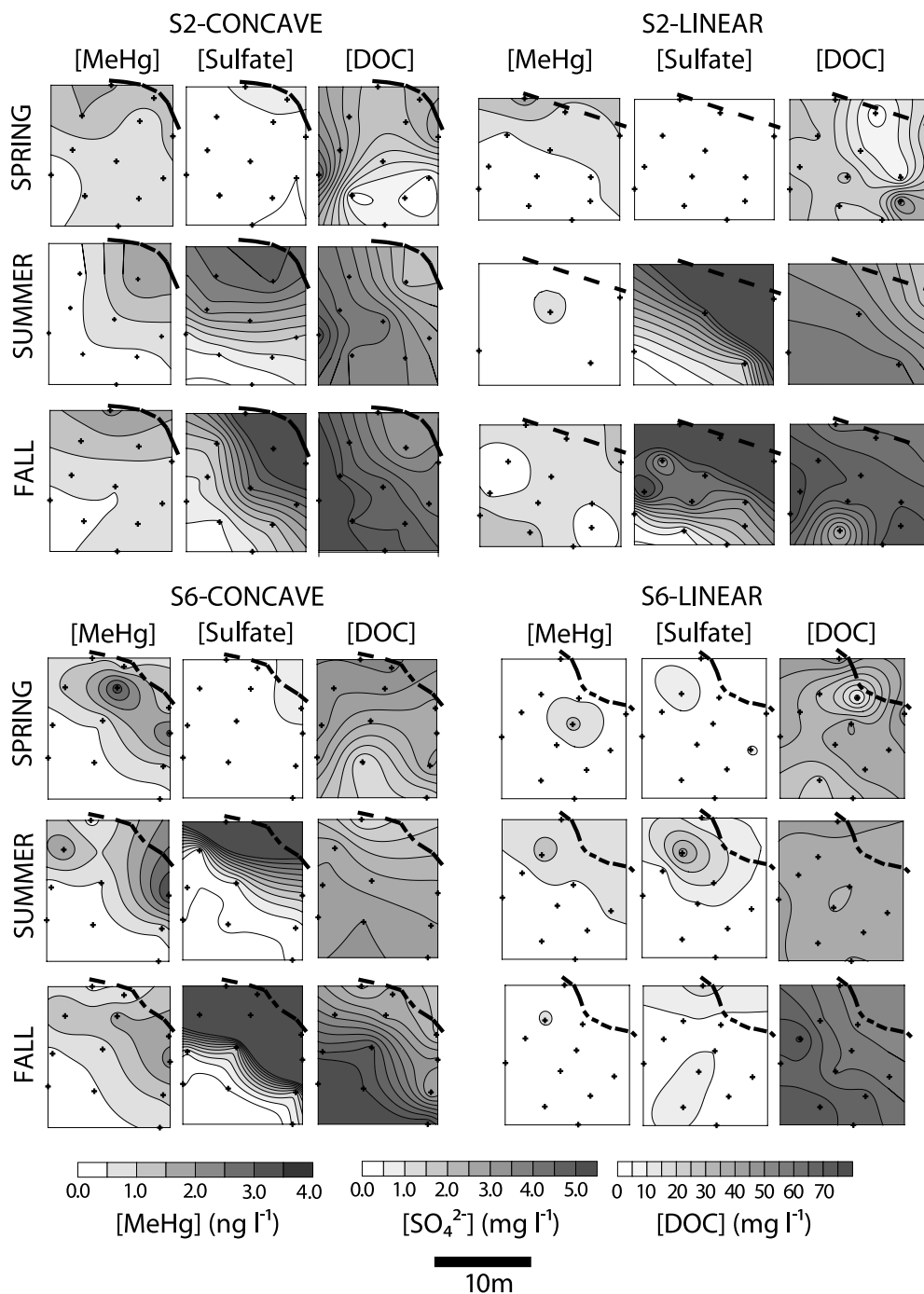


Figure 3. Spatial patterns of pore water MeHg, sulfate, and DOC concentration at the upland-peatland interface plots adjacent to where upland surface topography is concave (S2-CONCAVE and S6-CONCAVE) and where upland surface topography is linear (S2-LINEAR and S6-LINEAR). The dashed line in each represents the upland interface, and plots are approximately oriented in the same direction as shown in Figure 2. Fluxes from the upland are thus across the interface from the upper right of each plot toward the lower left.

twice as large as above S6-CONCAVE, but the pore water MeHg concentrations were higher in S6-CONCAVE. This could be the result of a combination of subtle factors such as differences in biogeochemical processing efficiency or because of unmeasured spatial or temporal variations in upland flux that are not attributable to topography. The simplest of explanations is that previous research [Mitchell *et al.*, 2008b]

has demonstrated that peatland S2 produces and exports considerably less MeHg than S6. This dissimilarity has been attributed to differences in reduction-oxidation conditions.

[20] Some upland soil water concentrations of MeHg (median = 0.17 ng l⁻¹; range < 0.02 to 0.45 ng l⁻¹; n = 5) were available at the same time as sampling for this study [Mitchell *et al.*, 2008b], but THg concentrations were not

because of difficulties in obtaining enough sample volume for analysis. In earlier work, the mean THg concentration in S2 upland interflow was 20.2 ng l^{-1} and in S6 upland interflow was 15.0 ng l^{-1} (Kolka, unpublished data, 1996). The low MeHg concentrations in upland runoff indicate that little Hg methylation occurs in upland soil water. Most importantly, upland fluxes of MeHg are insufficient to account for the pools of MeHg found in peatland pore waters at the upland-peatland interface. Thus the elevated concentrations of MeHg at the upland-peatland interface are due to in situ methylation or pore water accumulation and are not attributable to delivery from upland soils.

[21] Fluxes of inorganic mercury into the peatland margin may also have been an important control on MeHg production at the upland-peatland interface, but were not measured in this study. Hypothetically, if large amounts of inorganic mercury were transported from the upland hillslopes into the upland-peatland interface zone, one might expect that the production of MeHg would be affected, depending on the bioavailability of the introduced Hg [Barkay *et al.*, 1997; Benoit *et al.*, 1999]. Substantial quantities of inorganic Hg were certainly also delivered by runoff to the peatland margins during our study, however inorganic Hg fluxes were not likely the primary control on methylation for a number of reasons. In peatland mesocosms, the addition of a considerable amount of inorganic Hg (28 to 46 ng THg) in leaf litter leachate (as a proxy for upland runoff) did not result in measurable production of MeHg unless sulfate was also added [Mitchell *et al.*, 2008a]. Investigations of MeHg hot spots in these particular peatlands have shown very poor correlations between pore water THg and MeHg concentrations [Mitchell *et al.*, 2008b]. Most compelling to this argument was that whereas there were significant differences in the concentration of MeHg between the two types of upland-peatland topographic configurations in this study, pore water THg concentrations were not significantly different between the plots in either peatland S6 ($p = 0.408$) or peatland S2 ($p = 0.384$). This suggests that mercury methylation is not strongly related to the upslope delivery of inorganic mercury into these plots, but this does not discount a possible synergistic relationship between the focused runoff of inorganic mercury with sulfate and DOC, and the production of MeHg at the upland-peatland interface.

[22] Efficient sulfate reduction at the upland-peatland interface is demonstrated in the study plots. There is a rapid decrease in sulfate concentration from the upland interface into the peatland plots in summer and fall with considerably lower concentrations in spring (Figure 3). Apart from S6-LINEAR, the general patterns are similar among study plots, with high concentrations of sulfate extending approximately half of the distance across each study plot from the interface. After this, concentrations are considerably reduced within only a few meters. The rapid decrease in sulfate concentration was spatially coincident with zones of high MeHg concentration, especially within the upland-peatland interface plots that were situated below upland areas with concave topography (i.e., S6-CONCAVE AND S2-CONCAVE). Similar to previous work [Mitchell and Branfireun, 2005], this suggests that inputs of sulfate from the adjacent hillslope are efficiently reduced within the first 5 m of the upland-peatland interface zone. This area of efficient sulfate reduction appears to be optimal for the production of MeHg; not

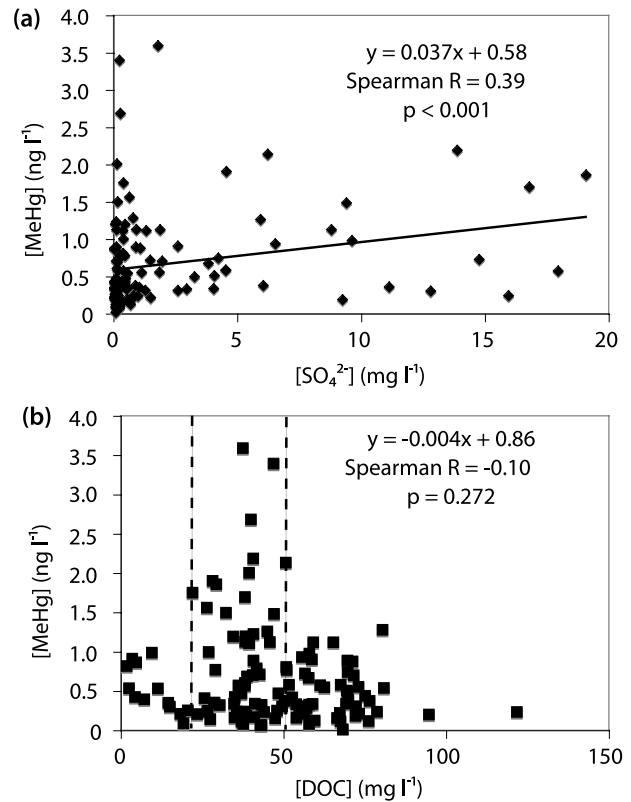


Figure 4. Relationships between MeHg concentration and (a) sulfate concentration and (b) dissolved organic carbon (DOC) concentration (dashed lines delineate the range in DOC corresponding to high MeHg concentration).

unexpected as MeHg production is closely coupled to sulfate reduction [Gilmour *et al.*, 1992; King *et al.*, 1999].

[23] Despite the relatively close spatial coincidence between decreases in sulfate concentration and increases in MeHg concentration, correlations between pore water sulfate and MeHg concentrations were weak (Figure 4). From this data, it appears that there is a small spatial lag between sulfate reduction and increases in pore water MeHg concentration. High concentrations of MeHg in pore water were observed across a broad range of sulfate concentrations. Although experimental additions of sulfate have been shown to stimulate the production of MeHg [Gilmour *et al.*, 1992; Branfireun *et al.*, 1999, 2001; Harmon *et al.*, 2004; Jeremiason *et al.*, 2006; Mitchell *et al.*, 2008a], it is likely that sulfate reduction and MeHg production are occurring along a hydrologic flow path and the concentrations of the two are not spatially coincident because of mass transfer.

[24] The patterns of DOC concentration in the sample plots were generally opposite to the patterns observed for sulfate concentrations (Figure 3). With only minor exceptions, DOC concentrations were generally lowest at the upland interface. Moreover, gradients in DOC concentration change over space were greater in the plots adjacent to topographically concave upland subcatchments. These patterns are indicative of a hydrologic influence from upland runoff on the geochemistry of the upland-peatland interface. Mean concentrations increased throughout the year from 31 mg l^{-1} in the spring, to 43 mg l^{-1} in the summer, and

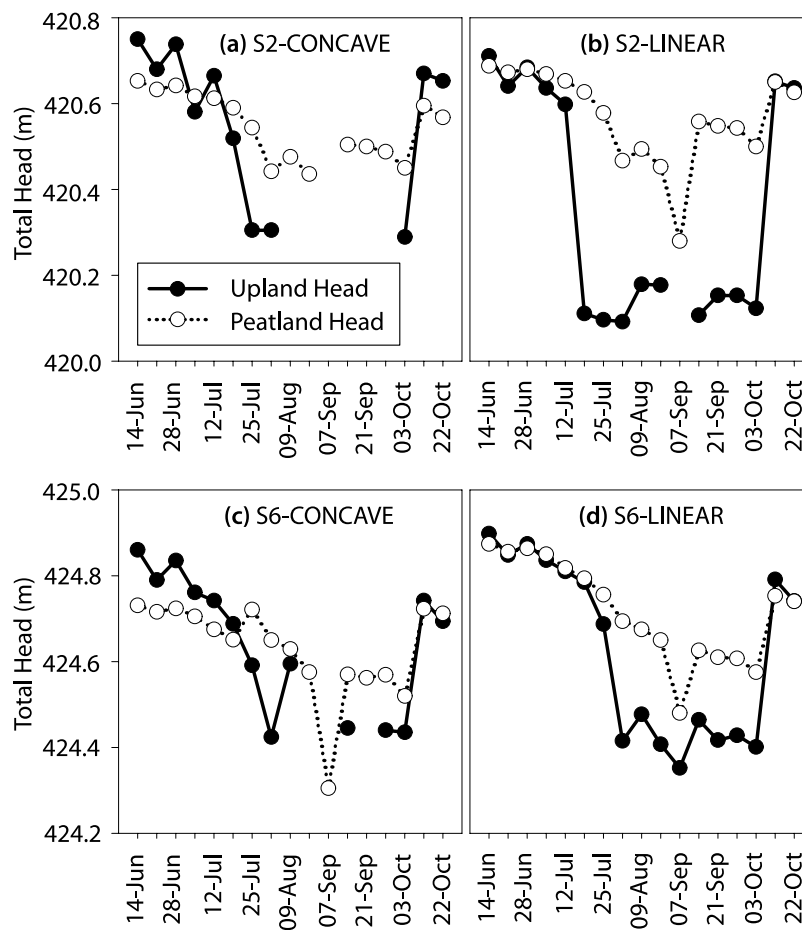


Figure 5. Total head (in meters above sea level) in upland and peatland wells across each upland-peatland interface study plot. When the upland water table is higher in elevation than that in the peatland water table, the direction of the water flux is toward the peatland.

to 63 mg l^{-1} in the fall. Concentrations in upland runoff were generally less than 20 mg l^{-1} . These patterns may thus be related to a dilution of peatland DOC by the flux of lower DOC concentration waters from the upland into the upland-peatland interface.

[25] A correlation between MeHg and DOC concentrations (Figure 4) was also not significant ($p = 0.27$), but did reveal that the highest MeHg concentrations only occurred over a range in DOC concentration between 22 and 50 mg l^{-1} . This lower overall range of DOC concentrations is closer to values observed in upland runoff, compared to peatland pore waters, and thus may be indicative of the upland runoff input. In previous research, it has been suggested that fluxes of labile carbon from upland hillslopes may stimulate increased MeHg production because mercury methylation in peatlands may be substrate-limited under conditions of increased sulfate input [Mitchell *et al.*, 2008a]. Although the relationship in Figure 4 is insignificant, the predominance of high MeHg concentrations at relatively low DOC concentrations suggest that upland DOC fluxes may indeed be more labile. Overall, the carbon controls on methylation appear to be complex because organic carbon quality is likely more important to mercury methylation and inorganic mercury bioavailability than is organic carbon quantity [Mitchell and Gilmour, 2008]. Further experimental research involving measures of organic

carbon bioavailability are necessary, but it remains possible that although DOC concentrations appear diluted at the upland-peatland interface because of lower DOC concentration runoff from the upland hillslope, the delivered DOC could still be considerably more labile than that produced in situ within the peatland.

3.3. Hydrogeochemical Differences Among Study Plots

[26] Over the study period, the hydraulic gradients from upland to peatland were positive during our spring and fall sampling in all plots (i.e., toward peatland), but negative during summer (Figure 5). Positive hydraulic gradients were maintained at the sites through June and into early July due to a relatively wet June with 111 mm of rainfall. During the spring sampling, hydraulic gradients across the S2-CONCAVE and S6-CONCAVE transects were 0.017 and 0.023, respectively. Comparatively, hydraulic gradients were approximately 6 times lower in the LINEAR plots (0.003 in S2-LINEAR and 0.004 in S6-LINEAR).

[27] In the summer, hydraulic gradients were negative across all transects as the July–August summer period was relatively dry with only 60 mm of rainfall. Although not apparent in the gradient data because measurements were only made weekly, there were exceptions to the direction of the hydraulic flux during the summer period. Small short-term fluxes of water from the upland organic horizon

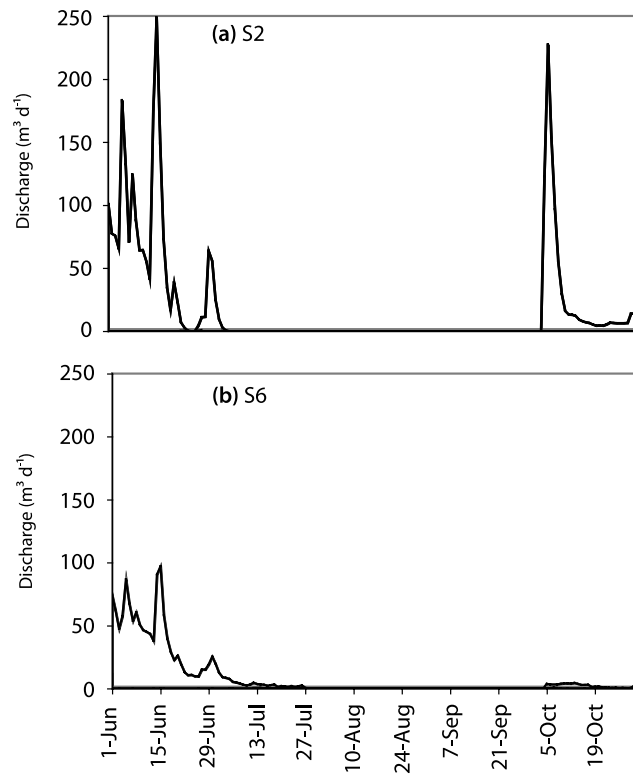


Figure 6. Discharge from watersheds (a) S2 and (b) S6 during the study period.

accumulated in the upland runoff collectors (therefore signifying a small flow from the upland into the peatland) following 3 summer storm events; an 11 mm event on 17 July, a 15 mm event on 9 August, and a 9 mm event on 17 August. Apart from these small event-based episodes, there was no apparent hydrologic connection from upland into peatland during the summer. Notably however, one of these short-term fluxes toward the peatland coincided with our midsummer sampling period. Because of the dry conditions, surface runoff from the peatlands ceased during the dry summer period (Figure 6). In peatland S2, flow ceased as of 7 July, but base flow conditions continued from peatland S6 until 31 July.

[28] The fate of water at the upland-peatland interface during the dry summer period is not known, but is likely lost to deeper seepage or to evapotranspiration. This dry summer period resulted in considerably lower water tables at the upland-peatland interface (depth > 10 cm below the surface at all sites) and the loss of a perched water table altogether in some upland wells. Apart from the short-duration summer upland fluxes described above, the upland-peatland hydrologic flux reversed during this period such that water from the peatland appeared to flow into the adjacent uplands. However, since the summer drop in upland head was greater (>0.4 m) than the depth of the A horizon (~0.3 m), it is unlikely that much peatland water would have been stored in the near-surface upland soils and later flowed back to the peatland in the fall. The relatively large drop in upland head suggests one of two possibilities for the movement of peatland water back to the upland. First, peatland water may have slowly seeped back into the deeper Koochiching Drift, where it would be lost to deep

seepage and evapotranspiration. It is also probable that due to the low permeability of the Koochiching Drift, little peatland water may have actually moved into the upland and the losses observed within the upland-peatland interface may have been due to downward vertical losses within the interface zone itself and to evapotranspiration.

[29] Following a 79 mm event from 4–5 October, surface runoff from both peatlands recommenced on 5 October. As a result of this event, the upland-peatland positive hydraulic gradient was restored. During our final sampling period, the hydraulic gradient across the S2-CONCAVE transect (0.014) was considerably steeper than across S2-LINEAR (<0.001). In the S6 watershed, the hydraulic gradient across S6-CONCAVE (0.003) was lower than across S6-LINEAR (0.006). Limited numbers of measurements make it difficult to determine if this difference is significant or persistent, but it may be due to contrasting antecedent moisture conditions between the two slopes. The much steeper slope across S6-CONCAVE may have been subjected to more extensive gravity drainage prior to the 5 October event. During the fall sampling under dry antecedent conditions, the increased soil water storage capacity in S6-CONCAVE had to be satisfied prior to the development of the saturated wedge. With this exception, upland-peatland hydraulic gradients were considerably steeper where upland topography was concave and subcatchment areas were larger.

[30] As a result of these hydraulic gradient characteristics, interflow fluxes of water from upland into peatland were, in general, greater from the concave and larger upland subcatchment areas (Figure 7). The fluxes have been integrated over a time period of 7 days, centered around only the sampling campaigns when the direction of the flux was toward the peatland (spring and fall), and only lateral fluxes are estimated. Although sampling was on a seasonal basis, this research does not strictly investigate seasonal variability, but rather hydrologic variability during three distinct periods. Between approximately 2 and 200 l wk⁻¹ of upland runoff flowed into each 10 m wide plot. These are relatively small volumes of runoff in comparison to the overall discharge from these watersheds. Our estimates of upland runoff were between 0.6 and 1.5% of watershed runoff over the same period in S2 and between 1.9 and 19% in S6. Despite the relatively small influxes of water from the surrounding upland, they appear to be significant given the observed statistical differences in MeHg concentrations in the study plots. This is likely due to the geochemical distinction between upland waters (oxic, sulfate and labile carbon laden) and peatland waters (anoxic, sulfate-poor, recalcitrant DOC).

[31] Given both the relatively large range in K_{sat} measurements in shallow soils of both watershed uplands (1×10^{-7} to $4 \times 10^{-5} \text{ m s}^{-1}$), and a limited number of replicates ($n = 7$ in S2; $n = 10$ in S6), the median K_{sat} in each watershed was used for calculating subsurface lateral flow in both upland-peatland plots. The median K_{sat} in both watersheds were similar ($4.1 \times 10^{-6} \text{ m s}^{-1}$ in S2; $4.7 \times 10^{-6} \text{ m s}^{-1}$ in S6). Given that spatial variabilities in K_{sat} between upland contributing areas in each watershed are not accounted for, water flux measurements are dependent only on hydraulic gradients. Also, the K_{sat} measurements more accurately estimate vertical K_{sat} . The calculations here therefore assume isotropy despite the potential for horizontal

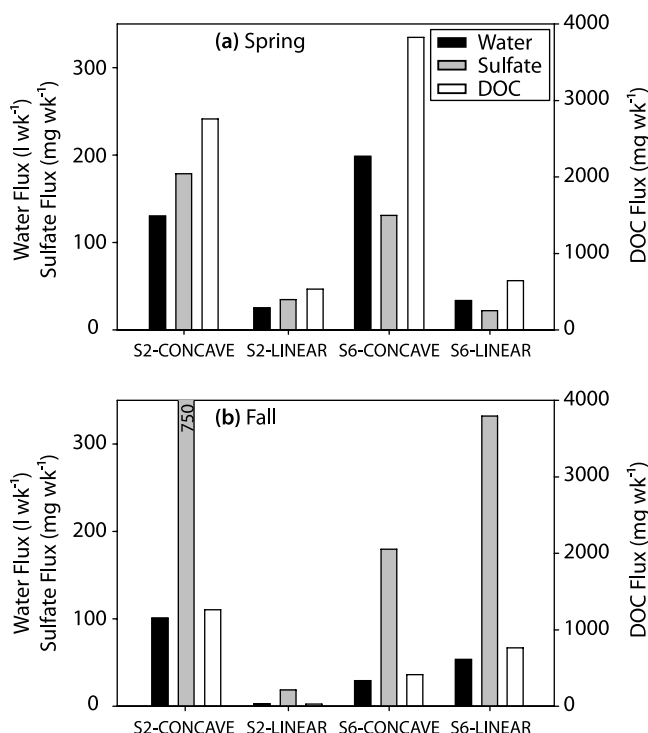


Figure 7. Upland fluxes of water, sulfate, and dissolved organic carbon (DOC), integrated over a 7-day period, into each peatland plot during the (a) spring and (b) fall sampling periods.

K_{sat} to be greater than vertical because of soil stratigraphic development and the presence of a layered organic horizon closer to the ground surface. It is thus possible that the lateral subsurface fluxes are underestimated, but almost certainly not overestimated. Further detailed work on the hillslope hydrologic processes governing event-scale lateral flow would improve the confidence around these estimates, but were beyond the scope of this study.

[32] Small differences in sulfate and DOC concentration were observed between watersheds, but mean concentrations from both plots in each watershed were used as small differences in concentrations are obfuscated by the magnitude of the water flux terms. In line with the estimates of water flux, the fluxes of DOC and sulfate were, in general, greater across CONCAVE upland-peatland transects than across LINEAR ones (Figure 7). These differences were most apparent in the spring sampling, when hydraulic gradients between upland and peatland were at their steepest. In the fall, when hydraulic gradients were shallower, upland fluxes into the S6-LINEAR plot were slightly more than fluxes into the S6-CONCAVE plot because of the lower hydraulic gradient at the latter plot explained earlier. Despite the estimated differences in upland flux, MeHg concentrations in the S6-CONCAVE plot remained elevated over those in the S6-LINEAR plot, suggesting that the limited water table data did not capture transient downslope water flows, or that water and solutes were transported via pathways that were not captured by the wells. This potential explanation is consistent with our hypothesis concerning the driving mechanisms for MeHg production at the upland-

peatland interface illustrated at other times of the year, but is unsubstantiated for this event.

3.4. Ecological Significance of Net Methylmercury Production Hot Spots in Upland-Peatland Watersheds

[33] From an ecosystem perspective, it is important to begin coupling these zones of elevated MeHg production and/or accumulation in the landscape to the fluxes of MeHg in peatland outlet waters that could impact organisms in downstream receiving waters. In conjunction with the measurement of spatial patterns of MeHg at the upland-peatland interface, MeHg fluxes from each watershed were calculated for the same periods as utilized in the above analyses. Fluxes from S2 were $7.5 \mu\text{g d}^{-1}$ (%-MeHg = 1.4%) during the spring sampling, $0 \mu\text{g d}^{-1}$ during the summer sampling as a result of a lowered water table and no water flow from the watershed, and $16 \mu\text{g d}^{-1}$ (%-MeHg = 1.3%) during the fall sampling. Fluxes from S6 were $48 \mu\text{g d}^{-1}$ (%-MeHg = 11%) during the spring, $0 \mu\text{g d}^{-1}$ during the summer as a result of no water flow from the watershed, and $3.1 \mu\text{g d}^{-1}$ (%-MeHg = 6.9%) during the fall. Fluxes were generally higher from peatland S6 and by far the highest during the spring, both coinciding with high concentrations of MeHg in pore waters at the upland-peatland interface. Under summer no-flow conditions, the magnitude of the in situ MeHg production is of no consequence to peatland MeHg export during that period; however there is evidence that MeHg produced in peatland soils may persist for some time, potentially even over the winter season as shown by high MeHg concentrations measured during the snowmelt period [Mitchell *et al.*, 2008c].

[34] At present, it is not clear how net MeHg production hot spots are physically coupled to the peatland or watershed outlet. The above temporal relations suggest that greater MeHg production at the upland-peatland interface is expressed at the peatland outlets on a seasonal basis. From a broad watershed perspective, hot spot formation at the upland-peatland interface is important because previous research has indicated that the outer peatland margin is the primary source area for surface water runoff from upland-peatland watersheds such as these [Urban *et al.*, 1989; Kolka *et al.*, 2001]. It is thus quite likely that the MeHg produced at upland-peatland interface hot spots is the dominant MeHg that is discharged from these watersheds to susceptible downstream aquatic ecosystems.

[35] Our study reveals that there is spatial variability in MeHg concentrations within the upland-peatland interface itself. With our current data, it is difficult to assess what happens to MeHg from a hot spot as it travels through the peatland toward the watershed outlet. Studies using enriched stable isotopes of mercury as tracers could elucidate these processes.

[36] Small-scale MeHg production hot spots, which may not be important to watershed discharge, may still be a significant source of MeHg exposure to biota at the hot spots themselves. Although much research on MeHg production is motivated by understanding the exposure risks to fish [Munthe *et al.*, 2006] and peatlands are generally not habitat for fish, hot spots could pose an elevated risk to insects, spiders, birds, and small mammals with localized foraging ranges.

[37] Finally, further research is warranted to understand whether relationships between topography, slope, and MeHg concentrations can be scaled to a larger landscape perspective. Recent advances in the availability of high-resolution topographic data, such as from light detection and ranging (LiDAR), may make it possible to predict zones of elevated MeHg production in watersheds at much broader scales. We note, however, that this possibility is likely to vary in relation to the degree to which hydrologic flow paths follow topography. In more northerly, boreal watersheds, these relationships are likely to be more easily detected because deep groundwater inputs are generally negligible, and surfaces are exposed bedrock or have shallow soils. Such conditions would lead to predominantly local, lateral hydrologic exchanges that follow topography relatively closely. In more deeply soiled watersheds where hydrologic flow paths are likely to be more complex, these same relationships may be less apparent.

4. Conclusions

[38] This is the first study to investigate from both a hydrologic and geochemical perspective why zones of high MeHg production and/or accumulation tend to form at the interface between peatland and upland and how variability in the intraecosystem fluxes of important reactants affects MeHg production and/or accumulation. Our data suggest that MeHg hot spots are spatially variable in relation to adjacent upland geomorphic form. Further, from a hydrologic perspective, these forms result in generally greater fluxes of sulfate and labile DOC, which are important reactants for sulfate reduction and hence Hg methylation. The empirical evidence generally supports this explanation, but some seasonal variability is evident that may be quite specific to hydrogeomorphic setting. Differences in hillslope antecedent moisture conditions between spring and fall sampling, differences in upland slope above study plots and/or small-scale spatial variability in flow paths during rewetting may explain the one inconsistency in the observations. Generally, the data presented here does support the hypothesis that pore water MeHg concentrations are greater at upland-peatland interfaces situated below concave upland hillslopes due to the delivery of sulfate-laden runoff to discrete, anoxic locations at the upland-peatland margin. Larger fluxes of sulfate promote the activity of sulfate-reducing bacteria and thus result in higher pore water MeHg concentrations. Upland-derived DOC is also likely more labile than peatland derived DOC [Mitchell et al., 2008a].

[39] These preliminary findings are particularly important because they demonstrate that watershed characteristics have a considerable influence on the biogeochemistry of peatlands, particularly in the formation of biogeochemical hot spots of MeHg production and/or accumulation along the upland-peatland interface. It therefore follows that changes or disturbances to the upland areas of watersheds may affect MeHg dynamics in peatlands. The control of upland topographic form on upland fluxes also suggests that new technologies such as high-resolution digital elevation models may aid in predicting the occurrence of important zones of MeHg production.

[40] The temporal variability of MeHg production at the upland-peatland interface is not easily coupled to MeHg export from these peatland basins. MeHg hot spots in the

summer do not have any impact on receiving waters during the summer because runoff from these watersheds ceases, however the longer-term behavior of the total pore water MeHg pool is unknown. Further research is necessary to conclusively link runoff source areas, MeHg production at the upland-peatland interface, peatland MeHg export, and the downstream contamination of susceptible organisms. In furthering our understanding of where MeHg hot spots form, we have provided a spatial framework from which others may investigate the in situ exposure of susceptible wildlife, such as birds, to areas of elevated MeHg production and/or accumulation.

[41] **Acknowledgments.** The authors wish to acknowledge the contributions of D. Kyllander and C. Dorrance (USFS) for field assistance at the Marcell Experimental Forest, M. Dalva and Tim Moore (McGill University) for the analysis of dissolved organic carbon samples, and S. Wanigaratne for laboratory assistance at the University of Toronto. We gratefully acknowledge improvements made to this paper by comments from D. Fitzgerald, C. Eckley, and L. Fenton. Comments from C. Driscoll, *Water Resour. Res.* editors, and two anonymous reviewers enhanced the quality of this paper. Financial support for this project was provided through a Natural Sciences and Engineering Research Council (NSERC) Discovery Grant to B.A.B. and an NSERC Canada Graduate Scholarship to C.P.J.M.

References

- Anderson, M. G., and T. P. Burt (1978), Role of topography in controlling throughflow generation, *Earth Surface Processes*, 3, 331–344.
- Barkay, T., M. Gillman, and R. R. Turner (1997), Effects of dissolved organic carbon and salinity on bioavailability of mercury, *Appl. Environ. Microbiol.*, 63, 4267–4271.
- Benoit, J. M., C. C. Gilmour, R. P. Mason, and A. Heyes (1999), Sulfide controls on mercury speciation and bioavailability to methylating bacteria in sediment pore waters, *Environ. Sci. Technol.*, 33, 951–959.
- Benoit, J. M., C. C. Gilmour, A. Heyes, R. P. Mason, and C. L. Miller (2003), Geochemical and biological controls over methylmercury production and degradation in aquatic ecosystems, *Am. Chem. Soc. Symp. Ser.*, 835, 262–297.
- Bloom, N. S. (1989), Determination of picogram levels of methylmercury by aqueous phase ethylation, followed by cryogenic gas chromatography with cold vapour atomic fluorescence detection, *Can. J. Fish. Aquat. Sci.*, 46, 1131–1140.
- Branfreun, B. A., N. T. Roulet, C. A. Kelly, and J. W. M. Rudd (1999), In situ sulphate stimulation of mercury methylation in a boreal peatland: Toward a link between acid rain and methylmercury contamination in remote environments, *Global Biogeochem. Cycles*, 13, 743–750.
- Branfreun, B. A., K. Bishop, N. T. Roulet, G. Granberg, and M. Nilsson (2001), Mercury cycling in boreal ecosystems: The long-term effect of acid rain constituents on peatland pore water methylmercury concentrations, *Geophys. Res. Lett.*, 28, 1227–1230.
- Brown, T. N., C. A. Johnston, and K. R. Cahow (2003), Lateral flow routing into a wetland: Field and model perspectives, *Geomorphology*, 53, 11–23.
- Compeau, G. C., and R. Bartha (1985), Sulfate-reducing bacteria: Principal methylators of mercury in anoxic estuarine sediment, *Appl. Environ. Microbiol.*, 50, 498–502.
- Gill, G. A., and W. F. Fitzgerald (1987), Picomolar mercury measurements in seawater and other materials using stannous chloride reduction and two-stage gold amalgamation with gas phase detection, *Mar. Chem.*, 20, 227–243.
- Gilmour, C. C., E. A. Henry, and R. Mitchell (1992), Sulfate stimulation of mercury methylation in fresh-water sediments, *Environ. Sci. Technol.*, 26, 2281–2287.
- Harmon, S. M., J. K. King, J. B. Gladden, G. T. Chandler, and L. A. Newman (2004), Methylmercury formation in a wetland mesocosm amended with sulfate, *Environ. Sci. Technol.*, 38, 650–656.
- Hedin, L. O., J. C. von Fischer, N. E. Ostrom, B. P. Kennedy, M. G. Brown, and G. P. Robertson (1998), Thermodynamic constraints on nitrogen transformations and other biogeochemical processes at soil-stream interfaces, *Ecology*, 79, 684–703.
- Horvat, M., L. Liang, and N. S. Bloom (1993), Comparison of distillation with other current isolation methods for the determination of methyl

- mercury compounds in low level environmental samples: part II. Water, *Anal. Chim. Acta*, 282, 153–168.
- Jeremiason, J. J., D. R. Engstrom, E. B. Swain, E. A. Nater, B. M. Johnson, J. E. Almendinger, B. A. Monson, and R. K. Kolka (2006), Sulfate addition increases methylmercury production in an experimental wetland, *Environ. Sci. Technol.*, 40, 3800–3806.
- King, J. K., F. M. Saunders, R. F. Lee, and R. A. Jahnke (1999), Coupling mercury methylation rates to sulfate reduction rates in marine sediments, *Environ. Toxicol. Chem.*, 18, 1362–1369.
- Kolka, R. K., D. F. Grigal, E. A. Nater, and E. S. Verry (2001), Hydrologic cycling of mercury and organic carbon in a forested upland-bog watershed, *Soil Sci. Soc. Am. J.*, 65, 897–905.
- McClain, M. E., et al. (2003), Biogeochemical hot spots and hot moments at the interface of terrestrial and aquatic ecosystems, *Ecosystems*, 6, 301–312.
- Mitchell, C. P. J., and B. A. Branfireun (2005), Hydrogeomorphic controls on reduction-oxidation conditions across boreal upland-peatland interfaces, *Ecosystems*, 8, 731–747.
- Mitchell, C. P. J., and C. C. Gilmour (2008), Methylmercury production in a Chesapeake Bay salt marsh, *J. Geophys. Res.*, 113, G00C04 doi:10.1029/2008JG000765.
- Mitchell, C. P. J., B. A. Branfireun, and R. K. Kolka (2008a), Assessing sulfate and carbon controls on net methylmercury production in peatlands: An in situ mesocosm approach, *Appl. Geochem.*, 23, 503–518.
- Mitchell, C. P. J., B. A. Branfireun, and R. K. Kolka (2008b), Spatial characteristics of net methylmercury production hot spots in peatlands, *Environ. Sci. Technol.*, 42, 1010–1016.
- Mitchell, C. P. J., B. A. Branfireun, and R. K. Kolka (2008c), Total mercury and methylmercury dynamics in upland-peatland watersheds during snowmelt, *Biogeochemistry*, 90, 225–241.
- Munthe, J., R. A. Bodaly, B. A. Branfireun, C. T. Driscoll, C. C. Gilmour, R. Harris, M. Horvat, M. Lucotte, and O. Malm (2006), Recovery of mercury-contaminated fisheries, *Ambio*, 36, 33–44.
- Nichols, D. S., and E. S. Verry (2001), Stream flow and ground water recharge from small forested watersheds in north central Minnesota, *J. Hydrol.*, 245, 89–103.
- Quinn, P., K. Beven, P. Chevallier, and O. Planchon (1991), The prediction of hillslope flow paths for distributed hydrological modeling using digital terrain models, *Hydrol. Processes*, 5, 59–79.
- Ratcliffe, H. E., G. M. Swanson, and L. J. Fischer (1996), Human exposure to mercury: A critical assessment of the evidence of adverse health effects, *J. Toxicol. Environ. Health*, 49, 221–270.
- Timmons, D. R., E. S. Verry, R. E. Burwell, and R. F. Holt (1977), Nutrient transport in surface runoff and interflow from an aspen-birch forest, *J. Environ. Qual.*, 6, 188–192.
- Urban, N. R., S. E. Bayley, and S. J. Eisenreich (1989), Export of dissolved organic carbon and acidity from peatlands, *Water Resour. Res.*, 25, 1619–1628.
- U.S. Environmental Protection Agency (2001), USEPA method 1630 (draft): Methyl mercury in water by distillation, aqueous ethylation, purge and trap, and CVAFS, *Publ. EPA-821-R-01-020*, 49 pp., Washington, D. C.
- U.S. Environmental Protection Agency (2002), USEPA method 1631, revision E: Mercury in water by oxidation, purge and trap, and cold vapour atomic fluorescence spectrometry for determination of mercury in aqueous samples, *Publ. EPA-821-R-02-019*, 46 pp., Washington, D. C.
- Verry, E. S., and D. R. Timmons (1982), Waterborne nutrient flow through an upland-peatland watershed in Minnesota, *Ecology*, 63, 1456–1467.
- Vidon, P., and A. R. Hill (2004), Denitrification and patterns of electron donors and acceptors in eight riparian zones with contrasting hydrogeology, *Biogeochemistry*, 71, 259–283.

B. A. Branfireun, Department of Geography, University of Toronto at Mississauga, 3359 Mississauga Road North, Mississauga, ON L5L 1C6, Canada.

R. K. Kolka, Northern Research Station, U.S. Department of Agriculture Forest Service, 1831 Highway 169 East, Grand Rapids, MN 55744, USA.

C. P. J. Mitchell, Department of Physical and Environmental Sciences, University of Toronto at Scarborough, 1265 Military Trail, Toronto, ON M1C 1A4, Canada. (carl.mitchell@utoronto.ca)